



# Horseradish peroxidase-mediated decolourization of Orange II: modelling hydrogen peroxide utilization efficiency at different pH values

Diego Alberto Morales Urrea<sup>1</sup> · Patricia Mónica Haure<sup>1,2</sup> · Fernando Sebastián García Einschlag<sup>3,4</sup> · Edgardo Martín Contreras<sup>1</sup>

Received: 17 January 2018 / Accepted: 25 April 2018 / Published online: 9 May 2018

© Springer-Verlag GmbH Germany, part of Springer Nature 2018

## Abstract

Enzymatic decolourization of azo-dyes could be a cost-competitive alternative compared to physicochemical or microbiological methods. Stoichiometric and kinetic features of peroxidase-mediated decolourization of azo-dyes by hydrogen peroxide (P) are central for designing purposes. In this work, a modified version of the Dunford mechanism of peroxidases was developed. The proposed model takes into account the inhibition of peroxidases by high concentrations of P, the substrate-dependant catalytic activity of peroxidases (e.g. the decomposition of P to water and oxygen), the generation of oxidation products (OP) and the effect of pH on the decolourization kinetics of the azo-dye Orange II (OII). To obtain the parameters of the proposed model, two series of experiments were performed. In the first set, the effects of initial P concentration (0.01–0.12 mM) and pH (5–10) on the decolourization degree were studied at a constant initial OII concentration (0.045 mM). Obtained results showed that at pH 9–10 and low initial P concentrations, the consumption of P was mainly to oxidize OII. From the proposed model, an expression for the decolourization degree was obtained. In the second set of experiments, the effect of the initial concentrations of OII (0.023–0.090 mM), P (0.02–4.7 mM), HRP (34–136 mg/L) and pH (5–10) on the initial specific decolourization rate ( $q_0$ ) was studied. As a general rule, a noticeable increase in  $q_0$  was observed for pHs higher than 7. For a given pH,  $q_0$  increased as a function of the initial OII concentration. Besides, there was an inhibitory effect of high P concentrations on  $q_0$ . To assess the possibility of reusing the enzyme, repeated additions of OII and P were performed. Results showed that the enzyme remained active after six reuse cycles. A satisfactory accordance between the change of the absorbance during these experiments and absorbances calculated using the proposed model was obtained. Considering that this set of data was not used during the fitting procedure of the model, the agreement between predicted and experimental absorbances provides a powerful validation of the model developed in the present work.

**Keywords** Horseradish peroxidase · Orange II · Hydrogen peroxide · Decolourization · Kinetic model

---

Responsible editor: Vitor Pais Vilar

---

**Electronic supplementary material** The online version of this article (<https://doi.org/10.1007/s11356-018-2134-8>) contains supplementary material, which is available to authorized users.

---

✉ Edgardo Martín Contreras  
edgardo.contreras@fi.mdp.edu.ar

<sup>1</sup> Instituto de Investigaciones en Ciencia y Tecnología de Materiales (INTEMA), CCT - Mar del Plata CONICET, Av. Juan B. Justo 4302 (7600), Mar del Plata, Argentina

<sup>2</sup> Facultad de Ingeniería, Universidad Nacional de Mar del Plata (UNMdP), Av. Juan B. Justo 4302 (7600), Mar del Plata, Argentina

<sup>3</sup> Instituto de Investigaciones Físicoquímicas Teóricas y Aplicadas (INIFTA), CCT - La Plata – CONICET, Diag 113 y 64 (1900), La Plata, Argentina

<sup>4</sup> Facultad de Ingeniería, Universidad Nacional de La Plata (UNLP), Av. 1 #750 (1900), La Plata, Argentina

## Introduction

Nowadays, azo-dyes account for about 70% of the world production of dyes (Rache et al. 2014). Because of the ease and cost effectiveness of their synthesis, and the stability and diversity of available colours, azo-dyes are widely used in many industries, such as textile, pharmaceutical, food manufacture, leather goods and others (Lin et al. 2014). More than 10% of dyes produced worldwide is lost in wastewaters during manufacture and application processes (Rauf and Ashraf 2012). Many synthetic azo-dyes and their metabolites are potentially toxic, carcinogenic and mutagenic (Sudha et al. 2014). Moreover, the discharge of non-treated textile industry wastewaters to aquatic ecosystems causes a reduction in sunlight penetration, which in turn decreases photosynthetic activity. Because this activity is an important source of dissolved oxygen, the presence of dyes in the aquatic systems leads to low dissolved oxygen conditions, causing a severe alteration to these ecosystems (Saratale et al. 2011). For this reason, the removal of colour from industrial wastewaters containing azo-dyes prior to their final discharge is crucial to protecting the receiving body water.

Several physicochemical methods, such as coagulation-flocculation (Lau et al. 2014), adsorption (Zhang et al. 2015), sonochemical decolourization (Dükkanci et al. 2014) and membranes (Mo et al. 2008), have been proposed for the removal of azo-dyes from wastewaters. Moreover, a wide range of advanced oxidation processes (AOP), such as the Fenton reaction (Doumic et al. 2013), Fenton-like reactions (Doumic et al. 2015; Inchaurredo et al. 2016), photo-Fenton (Zhou et al. 2016), electro-Fenton (Lin et al. 2014) and ozone (Tizaouia and Grima 2011), were also proposed. These methods are based on the generation in situ of strong oxidising species such as  $\text{OH}^*$  radicals, which are responsible for a sequence of reactions that breaks down the compounds into smaller and less harmful substances. Using appropriate conditions, several compounds can be completely mineralized into water and carbon dioxide. As a general rule, most of these methods are not economically viable due to the high requirements of energy (e.g. high reaction temperatures), chemicals (e.g. coagulants, hydrogen peroxide, ozone) and the generation of significant amounts of chemical sludge that may cause secondary pollution problems (Forgacs et al. 2004).

Biochemically assisted degradation processes are based on the metabolic potential of microorganisms or their enzymes to degrade a wide variety of compounds (Rauf and Ashraf 2012). The major drawback of using microorganisms is the fact that the removal process may take longer and is less predictable in comparison with physicochemical methods. Conversely, the use of enzymes instead of microorganisms is a simple way to obtain high removal rates of a specific compound under predictable conditions (Ali et al. 2013). Also, enzymatic degradation is preferred in cases where the target compound inhibits

the microbial growth. For this reason, enzymatic decolourization of azo-dyes could be an eco-friendly cost-competitive alternative compared to physicochemical or microbiological methods (Saratale et al. 2011; Rauf and Ashraf 2012). In particular, the use of peroxidases (e.g. soybean peroxidase, manganese peroxidase, lignin peroxidase, horseradish peroxidase) or their biomimetic systems (e.g. hematin) has been proposed to decolourise azo-dyes (Cheng et al. 2007; Franciscon et al. 2010; Ali et al. 2013; Chiong et al. 2016; Sahare et al. 2016; Cabrera et al. 2017).

Both stoichiometric and kinetic features of the peroxidase-mediated decolourization of azo-dyes by hydrogen peroxide are central for designing purposes. Many mathematical models regarding the effect of hydrogen peroxide, type of organic substrate, pH and others on the activity of peroxidases can be found in the literature. Although several reaction mechanisms of peroxidases can be found in the literature (Olsen et al. 2003; Gómez et al. 2008; Ali et al. 2013; Kalsoom et al. 2013), most of these models are modifications or extensions of the Dunford mechanism (Dunford and Stillman 1976).

## The Dunford mechanism

According to this mechanism, the first step of the catalytic cycle is the reaction between hydrogen peroxide (P) and the resting state of the enzyme ( $E_0$ ) to generate compound I ( $E_1$ ), which is two oxidising equivalents above  $E_0$ . Under the presence of a reducing substrate (S), two subsequent one-electron reduction steps of  $E_1$  occur. The first one-electron reduction step of  $E_1$  leads to the generation of compound II ( $E_2$ ), which is one oxidising equivalent above  $E_0$ . Finally, the second one-electron reduction step returns  $E_2$  to  $E_0$ . During each step, a radical species ( $S^*$ ) is produced due to the one-electron oxidation of the reducing substrate (S). The presence of these radicals results in a complex profile of reaction products that may include dimers, trimers and oligomers of the substrate (Chahbane et al. 2007; Gómez et al. 2008).

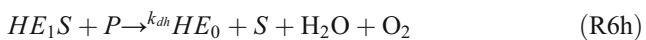
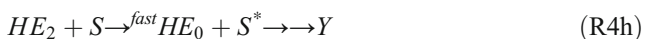
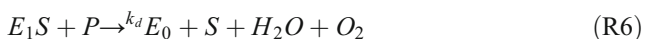
The form  $E_2$  can react with the excess of hydrogen peroxide (P) to produce an inactive form of the enzyme ( $E_3$ ), which can break down spontaneously to the native form ( $E_0$ ). This inactive form of the enzyme is responsible for the decrease of the reaction rate at high hydrogen peroxide concentrations. Moreover, the decay of  $E_3$  to  $E_0$  is associated with the catalytic activity of peroxidases (i.e. the conversion of hydrogen peroxide to oxygen and water) (Jakopitsch et al. 2005). An essential difference between the catalytic activity of catalases and peroxidases is that the latter depends on the presence of a reducing substrate (S). However, even in the absence of S, a residual, the catalytic activity of peroxidases can be observed. This residual catalytic activity is due to the presence of impurities

that might be present in the enzyme preparation or even the enzyme itself (Sahare et al. 2016).

### Modified Dunford mechanism

The model developed in the present work takes into account the inhibition of the enzymatic activity by high concentrations of hydrogen peroxide and the substrate-dependant catalatic activity of peroxidases (Nicell and Wright 1997; Jakopitsch et al. 2005; Sahare et al. 2016). To reduce the model complexity, the number of enzymatic species was kept as minimum as possible. Moreover, because short-term decolourization experiments under relatively low hydrogen peroxide concentrations were performed, the inactivation of the enzyme by hydrogen peroxide was considered negligible.

The proposed model also takes into account the effect of pH on the peroxidase activity reported by several authors (Satar and Husain 2009; Rauf and Ashraf 2012; Darwesh et al. 2016). As a general rule, pH is an essential environmental factor for all enzymes. pH affects the protonation degree of acid/base groups close to the active sites of the enzymes, changing their kinetic properties. Although a typical active site is usually composed by several groups with different  $pK_a$  values (Frey and Hegeman 2007), for modelling purposes it is usually assumed that the enzyme can be treated as a single acid/base system. Moreover, most acid/base reactions are quite fast. For this reason, it is usually assumed that the different configurations of the enzyme are in equilibrium (Tijskens et al. 2001). In this work, it was assumed that the tested enzyme had two pH-dependant states: non-dissociated (HE) or dissociated (E). According to all these considerations, the following reactions were proposed:



Reactions R1, R2, R5, R1h, R2h, and R5h are reversible, with  $K_P$ ,  $K_S$ ,  $K_I$ ,  $K_{Ph}$ ,  $K_{Sh}$ , and  $K_{Ih}$  being their respective equilibrium constants. To reduce the mathematical complexity, an instantaneous chemical equilibrium of these reactions was assumed. In other words, rates of reversible reactions are much higher than those corresponding to irreversible ones. Moreover, all dissociated and non-dissociated enzymatic species are related by acid/base equilibria, which are also considered to be instantaneously attained. In this work, the following equilibrium was considered:

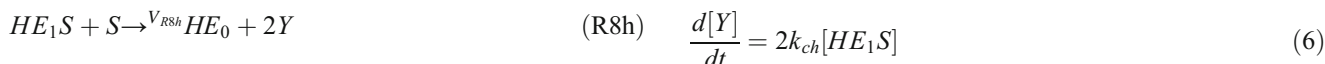


Acid/base equilibria corresponding to all other enzymatic forms can be deduced from appropriate combinations of R7 with the proposed reversible reactions. For this reason, only one acid/base equilibrium (e.g. R7) is necessary to completely define the distribution of all enzymatic species as a function of pH (see Supplementary Material, item 1).

Reactions R1 to R6 and R1h to R6h represent the reaction mechanism corresponding to the dissociated and undissociated states of the enzyme, respectively. The classic Dunford mechanism is represented by reactions R1 to R4 and R1h to R4h. Reactions R3 and R4 (R3h and R4h) are the one-electron reduction steps of the doubly oxidized form of the enzyme. Although the primary product of these reactions is  $S^*$ , these radicals may react to each other and also with dissolved oxygen yielding a complex profile of oxidation products (OP) (Lopez et al. 2004; Chahbane et al. 2007; Gómez et al. 2008). Moreover, the distribution of these OP (e.g. the relative amount of X and Y in the present model) could be a function of pH. For this reason, in the present model the species X and Y represent the set of oxidation products obtained during the oxidation of S under basic (R3, R4) or acidic (R3h, R4h) conditions, respectively. On the other hand, the inhibition of the enzymatic activity by P is represented by R5 and R5h. Finally, reactions R6 and R6h take into account the enzymatic decomposition of P (e.g. the catalatic activity of peroxidases). Because the presence of a reducing substrate (S) is necessary to produce the enzyme-substrate complex (R2, R2h), according to the proposed model the enzymatic decomposition of P only occurs under the presence of S (R6, R6h).

To simplify the number of enzymatic species, it was assumed that R4 and R4h are much faster than R3 and R3h, respectively. For this reason, concentrations of  $E_2$  and  $HE_2$  are negligible. Combining R3 with R4 and R3h with R4h,





Taking into account that R3 and R3h are the rate controlling steps of R8 and R8h, respectively,

$$V_{R8} = k_c[E_1S] \tag{1}$$

$$V_{R8h} = k_{ch}[HE_1S] \tag{2}$$

According to the above considerations, reaction rates corresponding to the reducing substrate (S), hydrogen peroxide (P) and the oxidation products (X, Y) are the following:

$$-\frac{d[S]}{dt} = 2k_c[E_1S] + 2k_{ch}[HE_1S] \tag{3}$$

$$-\frac{d[P]}{dt} = (k_c + 2k_d[P])[E_1S] + (k_{ch} + 2k_{dh}[P])[HE_1S] \tag{4}$$

$$\frac{d[X]}{dt} = 2k_c[E_1S] \tag{5}$$

The terms  $2k_d[P]$  and  $2k_{dh}[P]$  in Eq.(4) arises from the fact that one P is consumed during the production of E<sub>1</sub>S or HE<sub>1</sub>S (R2, R2h) while another P is consumed during its decomposition to water and molecular oxygen (R6, R6h). If the catalatic activity of the HRP is negligible ( $k_d = 0, k_{dh} = 0$ ), the proposed model is reduced to the classical Dunford mechanism in which one P can oxidize two S.

According to the above mentioned assumptions, the mass balance for the enzyme is

$$E_T = [E_0] + [E_1] + [E_1P] + [E_1S] + [HE_0] + [HE_1] + [HE_1P] + [HE_1S] \tag{7}$$

where  $E_T$  is the total enzyme concentration. Combining Eq.(7) with the definitions of the equilibrium constants and solving for  $[E_1S]$  (for details see Supplementary Material, item 1),

$$[E_1S] = E_T \frac{K_S K_P [S][P]}{\left(1 + \frac{H}{K_a}\right) + \left(K_P + K_{Ph} \frac{H}{K_a}\right)[P] + \left(K_P K_I + K_{Ih} K_{Ph} \frac{H}{K_a}\right)[P]^2 + \left(K_S K_P + K_{Sh} K_{Ph} \frac{H}{K_a}\right)[S][P]} \tag{8}$$

Besides, from the definitions of the equilibrium constants  $K_S, K_P, K_{Sh}, K_{Ph},$  and  $K_a$ , the ratio  $\frac{[HE_1S]}{[E_1S]}$  is

$$\frac{[HE_1S]}{[E_1S]} = \frac{K_{Sh} K_{Ph} H}{K_S K_P K_a} \tag{9}$$

Finally, substituting Eqs. (8) and (9) in Eqs. (3) to (6), reaction rates corresponding to S, P, X, and Y can be expressed as follows:

$$-\frac{d[S]}{dt} = 2 \left(k_c + k_{ch} \frac{K_{Sh} K_{Ph} H}{K_S K_P K_a}\right) E_T \frac{K_S K_P [S][P]}{\left(1 + \frac{H}{K_a}\right) + \left(K_P + K_{Ph} \frac{H}{K_a}\right)[P] + \left(K_P K_I + K_{Ih} K_{Ph} \frac{H}{K_a}\right)[P]^2 + \left(K_S K_P + K_{Sh} K_{Ph} \frac{H}{K_a}\right)[S][P]} \tag{10}$$

$$-\frac{d[P]}{dt} = \left[(k_c + 2k_d[P]) + (k_{ch} + 2k_{dh}[P]) \frac{K_{Sh} K_{Ph} H}{K_S K_P K_a}\right] E_T \frac{K_S K_P [S][P]}{\left(1 + \frac{H}{K_a}\right) + \left(K_P + K_{Ph} \frac{H}{K_a}\right)[P] + \left(K_P K_I + K_{Ih} K_{Ph} \frac{H}{K_a}\right)[P]^2 + \left(K_S K_P + K_{Sh} K_{Ph} \frac{H}{K_a}\right)[S][P]} \tag{11}$$

$$\frac{d[X]}{dt} = 2k_c E_T \frac{K_S K_P [S][P]}{\left(1 + \frac{H}{K_a}\right) + \left(K_P + K_{Ph} \frac{H}{K_a}\right)[P] + \left(K_P K_I + K_{Ih} K_{Ph} \frac{H}{K_a}\right)[P]^2 + \left(K_S K_P + K_{Sh} K_{Ph} \frac{H}{K_a}\right)[S][P]} \tag{12}$$

$$\frac{d[Y]}{dt} = 2k_{ch} \frac{K_{Sh} K_{Ph} H}{K_S K_P K_a} E_T \frac{K_S K_P [S][P]}{\left(1 + \frac{H}{K_a}\right) + \left(K_P + K_{Ph} \frac{H}{K_a}\right)[P] + \left(K_P K_I + K_{Ih} K_{Ph} \frac{H}{K_a}\right)[P]^2 + \left(K_S K_P + K_{Sh} K_{Ph} \frac{H}{K_a}\right)[S][P]} \tag{13}$$

## Materials and methods

### Chemicals and reagents

Analytical grade (>98%) Orange II (OII) sodium salt (CAS number 633-96-5) and horseradish peroxidase (HRP) type I (CAS number 9003-99-0) were from Sigma-Aldrich. Both compounds are widely referenced as model compounds for peroxidases and azo-dyes, respectively (Chahbane et al. 2007; Sudha et al. 2014; Zhang et al. 2015). Orange II was used without further purification. The enzyme was supplied as lyophilized powder. According to the manufacturer, the specific activity was 146 units/mg of the solid powder (one unit corresponds to the amount of enzyme that forms 1 mg of purpurogallin from pyrogallol in 20 s at pH 6 and 20 °C). All other salts used in this work were of reagent grade from Anedra (San Fernando, Argentina).

### Experimental setup and methods

Decolourization assays were performed in 3-mL quartz spectrophotometric cells at room temperature ( $22 \pm 2$  °C). Appropriate amounts of HRP were diluted in a phosphate buffer (100 mM) at the studied pH (5 to 10) to obtain 37 to 150 mgHRP L<sup>-1</sup>. Orange II (0.5 to 2 mM) and hydrogen peroxide (0.25 to 100 mM) stock solutions were prepared using the abovementioned phosphate buffer. A typical assay was as follows: 2 mL of HRP and 100 µL of OII were poured into the spectrophotometric cell; then, the reaction was started with the addition of 100 µL of hydrogen peroxide. According to this procedure, initial concentrations in the reaction mixture were 34–136 mg/L of enzyme (E), 0.02–0.1 mM of OII (S), and 0.02–4.7 mM of hydrogen peroxide (P). At appropriate time intervals, UV/Vis spectra were recorded using a spectrophotometer Shimadzu UV-1800. In some experiments, absorbance measurements were performed at 485 nm; in these cases, data were recorded at 1 data/s. The relationship between the absorbance at 485 nm (A, a.u.) and OII concentration was linear within the tested range of the dye concentration. The molar attenuation coefficient of OII at 485 nm ( $\epsilon_{OII}$ ) was  $19.5 \pm 0.3$  a.u. cm<sup>-1</sup> mM<sup>-1</sup>. The initial decolourization rate ( $V_{D0}$ , a.u. min<sup>-1</sup>) was obtained from the slope of the linear portion of A as a function of time (t, min). Then, the initial specific decolourization rate ( $q_0$ , a.u. min<sup>-1</sup> L<sup>-1</sup> mgE<sup>-1</sup>) was calculated as the ratio between  $V_{D0}$  and the total enzyme concentration ( $E_T$ , mgE L<sup>-1</sup>) in the reaction mixture. Under the tested conditions, the decolourization of OII by hydrogen peroxide was negligible. Moreover, the decomposition of hydrogen peroxide by HRP in the absence of OII was negligible. At 4 °C, stock HRP solutions were stable for about 1 week. All dynamic simulations and fits of the developed equations to the experimental data were performed using SigmaPlot for Windows 10.0 (Systat Software, Inc.).

## Results and discussion

### Changes on the UV/Vis spectrum of OII as a function of time

Figure 1 shows the molar attenuation coefficient ( $\epsilon$ ) at pH 7 corresponding to OII (Fig. 1a), the HRP employed in the present work (Fig. 1b) and hydrogen peroxide (Fig. 1c). Within the visible region, OII exhibits two absorption bands at 485 and 430 nm, which correspond to its hydrazone and azo-tautomeric forms, respectively (Fig. 1a). The other two bands at 230 and 310 nm are related with benzene and naphtalene rings of OII (Li et al. 2014; Zhou et al. 2016). Because pKa of OII is 11.4 (Oakes and Gratton 1998), similar UV/Vis spectra

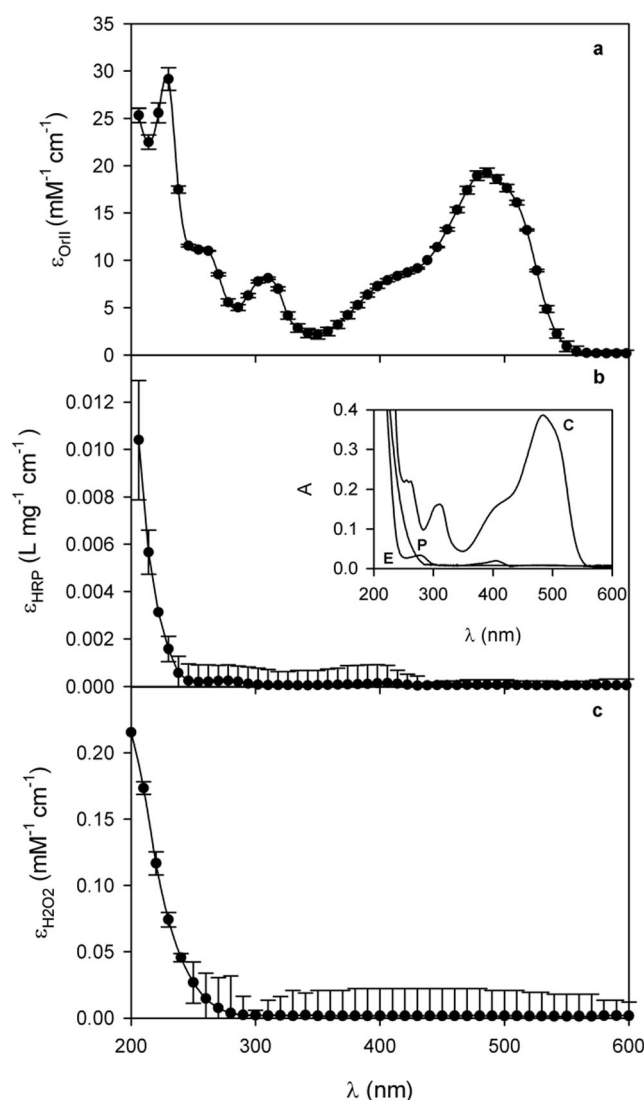


**Fig. 1** Molar attenuation coefficient ( $\epsilon$ ) at pH 7 in phosphate buffer (100 mM) as a function of wavelength ( $\lambda$ ) corresponding to **a** Orange II, **b** HRP and **c** hydrogen peroxide. Bars indicate the 95% confidence interval. Inset: UV/Vis spectra of OII (0.02 mM), HRP (136 mgE L<sup>-1</sup>) and hydrogen peroxide (4.7 mM)

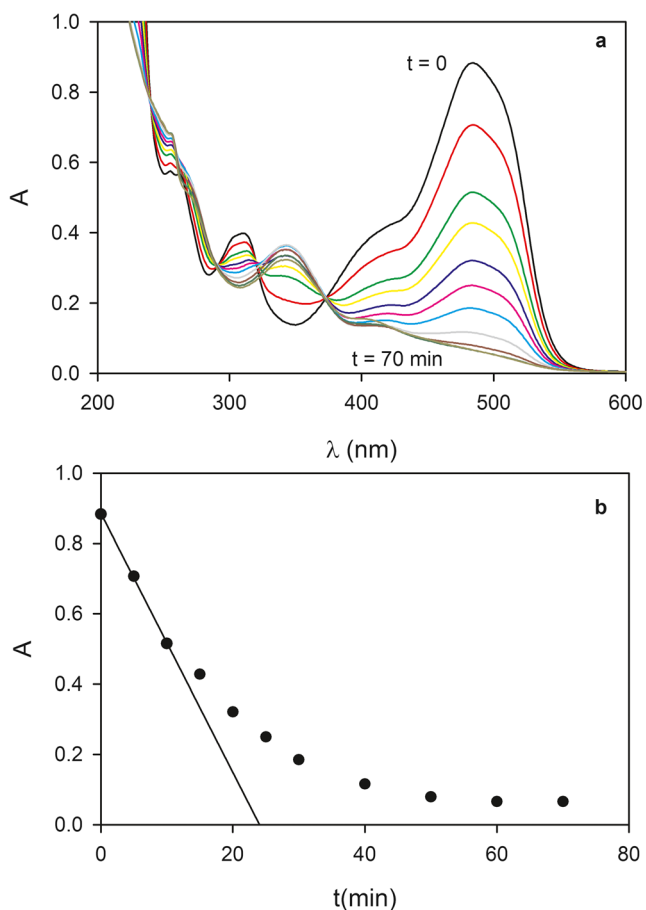


**Fig. 2** **a** UV/Vis spectral changes during a typical decolourization experiment. Tested conditions: OII = 0.045 mM, hydrogen peroxide = 0.090 mM, HRP = 136 mgE L<sup>-1</sup>, pH = 6. **b** Absorbance at 485 nm as a function of time. Continuous line indicates the linear regression of the first data; the slope corresponds to the initial decolourization rate ( $V_{0D}$ ) at the tested conditions

were obtained within the tested pH range (5 to 10). Considering the highest initial peroxide and enzyme concentrations tested ( $P_0 = 4.7$  mM,  $E = 136$  mgE L<sup>-1</sup>), and according to the molar attenuation coefficients depicted in Figs. 1b, c, the calculated contribution of hydrogen peroxide and HRP to the total absorbance at 485 nm was less than 0.01 a.u. These low absorbance values were negligible in comparison with those corresponding to the lowest tested dye concentration (Fig. 1, inset). For this reason, the absorbance at 485 nm was employed to follow the OII concentration as a function of time. A similar approach was used by other authors (Rache et al. 2014).

Figure 2a shows the change of UV/Vis spectra corresponding to a typical decolourization experiment. As a general rule, a decrease of the above mentioned OII characteristic absorbance bands within the visible region was observed. Then, as the reaction proceeds, a new absorption band at 340 nm appeared due to the formation of OII oxidation products (OP). Figure 2b shows that the absorbance

at 485 nm decreased as a function of time up to a given final value ( $A_f$ ). To verify if the reaction stopped due to oxidant depletion, hydrogen peroxide was added to the reaction mixture. Nevertheless, absorbance values were constant, suggesting that hydrogen peroxide were in excess with respect to OII and that this final absorbance was due to the presence of OP that cannot be further oxidized by hydrogen peroxide under the tested conditions.

The occurrence of refractory intermediates for the enzyme-mediated OII decolourization was reported by other authors. Lopez et al. (2004) demonstrated that the main oxidation products (OP) of OII by a manganese peroxidase were 4-diazoniumbenzenesulphonate and 4-hydroxybenzenesulphonate. Besides, other minor OPs such as 4-aminobenzenesulphonate and 1,2-naphthoquinone were also reported. Chahbane et al. (2007) studied the oxidation of OII by hydrogen peroxide catalyzed by a hemin-based biomimetic model of peroxidases in aqueous solutions. Those authors reported the presence of phthalic acid and 4-hydroxybenzenesulphonate from the non-enzymatic oxidation of 1,2-naphthoquinone and 4-diazoniumbenzenesulphonate, respectively. Recently, Cabrera et al. (2017) reported the following OP during the oxidation of OII by hydrogen peroxide catalyzed by hematin (a biomimetic system for HRP): 1-amino 2-naphtol, sulphanilate, 1-diazo 2-naphtol, 1,2-napthoquinone, 4-hydroxybenzenesulphonate, 4-diazobenzenesulphonate and aniline.

### Stoichiometry of the HRP-mediated decolourization reaction of OII by hydrogen peroxide ( $Y_{P/S}$ )

The amount of hydrogen peroxide required for the decolourization of a given dye ( $Y_{P/S}$ ) mediated by a HRP is a key parameter in the design of colour removal systems. As a general rule, when hydrogen peroxide is used as a bleaching agent of coloured wastewaters, hydrogen peroxide is consumed in bleaching (R3, R3h, R4, R4h) as well as in self-decomposition reactions (R6, R6h). Efficient hydrogen peroxide consumption depends on the relative rates of these reactions, which in turn may depend on several factors, such as pH and hydrogen peroxide and dye initial concentrations. In this section, the observable stoichiometry of the HRP-mediated decolourization reaction of OII by hydrogen peroxide ( $Y_{P/S}$ ) is discussed.

In the present model, it was assumed that the absorbance at 485 nm ( $A$ ) of the reaction mixture depended on the dye concentration (Rache et al. 2014) and on the obtained oxidation products:

$$A = \varepsilon_S[S] + \varepsilon_X[X] + \varepsilon_Y[Y] \quad (14)$$

where  $\varepsilon_S$ ,  $\varepsilon_X$  and  $\varepsilon_Y$  are the molar attenuation coefficients of  $S$ ,  $X$  and  $Y$ , respectively. Because  $X$  and  $Y$  represent a mixture of

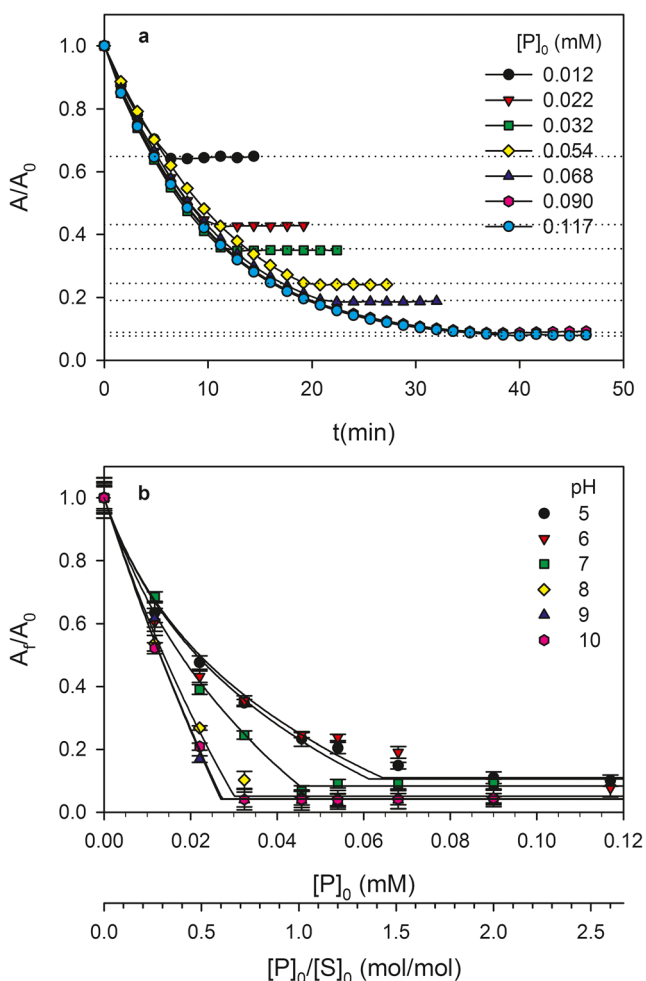


**Fig. 3** **a** Example of the effect of time and the initial hydrogen peroxide concentration ( $P_0$ ) on the ratio  $A/A_0$ ; in this example,  $\text{pH} = 6$ . **b** Effect of  $P_0$  and  $\text{pH}$  on the ratio  $A/A_0$ . In all cases,  $[S]_0 = 0.045 \text{ mM}$ . Bars represent the standard deviation. Lines in **b** represent the fitting results of Eq. (27) to the experimental data

products obtained at basic or acidic conditions,  $\epsilon_X$  and  $\epsilon_Y$  are apparent molar attenuation coefficients. From the ratio between Eqs.(12), (13) and (10), the concentrations of  $S$ ,  $X$  and  $Y$  can be related as follows:

$$-\frac{d[X]}{d[S]} = \frac{k_c}{k_c + k_{ch} \frac{K_{HS}K_{HP}}{K_S K_P} \frac{H}{K_a}} = \frac{K_{ap}}{K_{ap} + H} \quad (15)$$

$$-\frac{d[Y]}{d[S]} = \frac{k_{ch} \frac{K_{HS}K_{HP}}{K_S K_P} \frac{H}{K_a}}{k_c + k_{ch} \frac{K_{HS}K_{HP}}{K_S K_P} \frac{H}{K_a}} = \frac{H}{K_{ap} + H} \quad (16)$$

where  $K_{ap} = K_a \frac{K_S K_P}{K_{HS} K_{HP}} \frac{K_S K_P}{K_{HS} K_{HP}}$  is an apparent dissociation constant. Taking into account that the decolourization assays were performed at a constant  $\text{pH}$  and that the reaction mixture at the beginning of the experiment is devoid of OP ( $[X]_0 = [Y]_0 =$

0), from the integration of Eqs. (15) and (16), the following expressions were obtained:

$$[X] = \frac{K_{ap}}{K_{ap} + H} ([S]_0 - [S]) \quad (17)$$

$$[Y] = \frac{H}{K_{ap} + H} ([S]_0 - [S]) \quad (18)$$

where  $[S]_0$  is the initial concentration of the reducing substrate. Then, combining Eqs. (14), (17) and (18), the ratio  $A/A_0$  is

$$\frac{A}{A_0} = \frac{[S]}{[S]_0} + r_f \frac{([S]_0 - [S])}{[S]_0} \quad (19)$$

with

$$r_f = r_{fOH} \left( \frac{K_{ap}}{K_{ap} + H} \right) + r_{fH} \left( \frac{H}{K_{ap} + H} \right) \quad (20)$$

where  $r_{fOH} = \frac{\epsilon_X}{\epsilon_S}$  and  $r_{fH} = \frac{\epsilon_Y}{\epsilon_S}$  are the  $r_f$  values obtained under basic or acidic conditions, respectively. Because  $[S]$  changes as a function of time, the ratio  $A/A_0$  changes also (Fig. 3a). However, for sufficient long times, this ratio tends to constant value  $A_f/A_0$  indicating that the decolourization reaction stopped. Moreover, Fig. 3b shows that for a given  $\text{pH}$ , the ratio  $A_f/A_0$  decreased as the initial concentration of  $P$  increased up to a certain value. Then, further increases of  $P$  did not produce higher reductions of the ratio  $A_f/A_0$ , suggesting that under these conditions hydrogen peroxide was in excess with respect to  $S$  (Fig. 3b).

According to Eq. (19), the lowest  $A_f/A_0$  ratio that can be achieved corresponds to the complete removal of  $S$  ( $[S]_f = 0$ ). Thus, under the excess of  $P$  with respect to  $S$ ,

$$\frac{A_{\min}}{A_0} = r_f \quad (21)$$

Conversely, under the excess of  $S$  with respect to  $P$ , hydrogen peroxide is completely consumed ( $[P]_f = 0$ ). However, a given final concentration of the reducing substrate ( $[S]_f$ ) still remains in solution. Under the latter condition, the ratio between Eqs. (11) and (10) allows the calculation of  $[S]_f$  as follows:

$$\frac{d[P]}{d[S]} = \frac{1}{2} + \alpha [P] \quad (22)$$

with

$$\alpha = \frac{\left( k_d + k_{dh} \frac{K_{Sh}K_{Ph}}{K_S K_P} \frac{H}{K_a} \right)}{\left( k_c + k_{ch} \frac{K_{Sh}K_{Ph}}{K_S K_P} \frac{H}{K_a} \right)} = \alpha_{OH} \left( \frac{K_{ap}}{K_{ap} + H} \right) + \alpha_H \left( \frac{H}{K_{ap} + H} \right) \quad (23)$$

where  $\alpha_{OH} = \frac{k_d}{k_c}$  and  $\alpha_H = \frac{k_{dh}}{k_{ch}}$  are the values of  $\alpha$  ( $\text{mM}^{-1}$ ) obtained at basic and acidic conditions, respectively.

**Table 1** Fitting results of Eqs. (20), (23) and (27) to the data shown in Fig. 3b

Coefficient	Units	Value
$r_{fOH}$	Dimensionless	$0.041 \pm 0.008$
$r_{fH}$	Dimensionless	$0.12 \pm 0.01$
$\alpha_{OH}$	$\text{mM}^{-1}$	$8 \pm 2$
$\alpha_H$	$\text{mM}^{-1}$	$41 \pm 2$
$K_{ap}$	M	$(6 \pm 2) \times 10^{-8}$

According to Eq. (23), if the decolourization reaction is performed under constant pH,  $\alpha$  is a constant also. Thus, the integration of Eq. (22) yields the following expression:

$$[S]_0 - [S]_f = \frac{1}{\alpha} \ln \left( \frac{1 + 2\alpha[P]_0}{1 + 2\alpha[P]_f} \right) \tag{24}$$

Based on Eq. (24), the minimum initial concentration of P ( $[P]_C$ ) that is necessary to completely remove S ( $[S]_f = 0$ ,  $[P]_f = 0$ ) can be obtained from Eq. (24):

$$[P]_C = \frac{1}{2\alpha} \left( e^{\alpha[S]_0} - 1 \right) \tag{25}$$

In the cases when  $[P]_0 < [P]_C$  (e.g. under the excess of S),  $[P]_f = 0$ . Then, combining Eqs. (19) and (24),

$$\frac{A_f}{A_0} = 1 - (1 - r_f) \frac{1}{\alpha[S]_0} \ln(1 + 2\alpha[P]_0) \tag{26}$$

According to Eq. (26), under the excess of S, the ratio  $\frac{A_f}{A_0}$  decreases as  $[P]_0$  increases. However, when  $[P]_0 < [P]_C$ ,  $[S]_f = 0$  and a further decrease of the ratio  $\frac{A_f}{A_0}$  cannot be achieved (Eq. 21). Considering Eqs. (21), (25) and (26),

$$\frac{A_f}{A_0} = \begin{cases} 1 - (1 - r_f) \frac{1}{\alpha[S]_0} \ln(1 + 2\alpha[P]_0) & [P]_0 < [P]_C \\ r_f & [P]_0 \geq [P]_C \end{cases} \tag{27}$$

where  $r_f$  (Eq. 20) and  $\alpha$  (Eq. 23) are a function of pH.

Equations (20), (23) and (27) were fitted to the experimental data shown in Fig. 3b to obtain the coefficients  $r_{fOH}$ ,  $r_{fH}$ ,  $\alpha_{OH}$ ,  $\alpha_H$  and  $K_{ap}$ ; fitting results are shown in Table 1. According to Eq. (23),  $\alpha$  ranges from  $\alpha_{OH} = 8 \text{ mM}^{-1}$  ( $\text{pH} > \text{pK}_{ap}$ ) to  $\alpha_H = 41 \text{ mM}^{-1}$  ( $\text{pH} < \text{pK}_{ap}$ ). The coefficient  $\alpha$  is a measure of the ratio between the consumption of P due to HRP catalytic activity through reactions (R6, R6h) and HRP decolourization activity through reactions (R3, R3h). Table 1 demonstrates that the contribution of the decomposition reaction to the total consumption of P decreases as pH increase (for more details, see the Supplementary Material, item 2).

The coefficient  $r_f$  represents the lower value of the ratio  $A_f/A_0$  that can be achieved under the excess of peroxide

(Eq. 21). According to Table 1, this minimum absorbance ratio ranges from 0.04 to 0.12 at basic ( $\text{pH} > \text{pK}_{ap}$ ) or acid ( $\text{pH} < \text{pK}_{ap}$ ) conditions, respectively. Thus, from a practical standpoint, these results can help to predict the maximum decolourization degree at a given pH value. Figure 3b shows that for pH values higher than 7 and using an initial ratio  $P_0/S_0 > 0.6 \text{ mol/mol}$ , a maximum decolourization degree of about 95% was obtained. Similar results were reported by López (2005), who studied the decolourization of OII by a manganese peroxidase finding a decolourization degree between 80 and 90% when the ratio  $P_0/S_0$  was about 1 mol/mol. Increasing the ratio  $P_0/S_0$  does not result in higher decolourization degrees. For example, Chiong et al. (2016) studied the decolourization of methyl orange dye solutions by peroxidases from extracted from bio-wastes of soybean hulls and luffa (*Luffa acutangula*) skin peels. Those authors reported a maximum decolourization degree 81% with the soybean peroxidase using a ratio  $P_0/S_0 = 22 \text{ mol/mol}$ , which is about 35 times higher than that used in the present work.

By definition, the observable stoichiometric coefficient for the HRP-mediated decolourization reaction of OII ( $Y_{P/S}$ ) is the amount of P consumed per unit of dye (S) decolourized:

$$Y_{P/S} = \frac{[P]_0 - [P]_f}{[S]_0 - [S]_f} \tag{28}$$

where the subindex 0 and  $f$  indicate initial and final concentrations, respectively.

From the experimental ratio  $A_f/A_0$  and rearranging Eq. (19), the term  $[S]_0 - [S]_f$  was obtained. In the cases when  $[P]_0 < [P]_C$ ,  $[P]_f = 0$ . Conversely, when  $[P]_0 \geq [P]_C$ , by definition  $[S]_f = 0$ ; in this case,  $[P]_f$  was obtained from Eq. (24) using the coefficients depicted in Table 1. Then, in both cases  $Y_{P/S}$  was calculated using Eq. (28). Besides, from the knowledge of  $\alpha$ , the observable stoichiometric coefficient for the HRP-mediated decolourization reaction of OII ( $Y_{P/S}$ ) can be calculated as follows (for more details, see Supplementary Material, item 3):

$$Y_{P/S} = \begin{cases} \frac{\alpha[P]_0}{\ln(1 + 2\alpha[P]_0)} & [P]_0 < [P]_C \\ \frac{[P]_0 - \frac{1}{2\alpha} \left[ (1 + 2\alpha[P]_0) e^{-\alpha[P]_0} - 1 \right]}{[S]_0} & [P]_0 \geq [P]_C \end{cases} \tag{29}$$

where  $[P]_C$  is given by Eq. (26).

According to the classical Dunford mechanism (Fig. 4, dotted line), 2 mol of the reducing compound (e.g. OII in the present work) is oxidized per mole of hydrogen peroxide consumed, which corresponds to  $Y_{P/S} = 0.5 \text{ mol/mol}$ . Figure 4 shows that for pH values between 9 and 10,  $Y_{P/S}$  ranged from 0.5 to 1.2 mol/mol. Conversely, for pH 5 to 8,



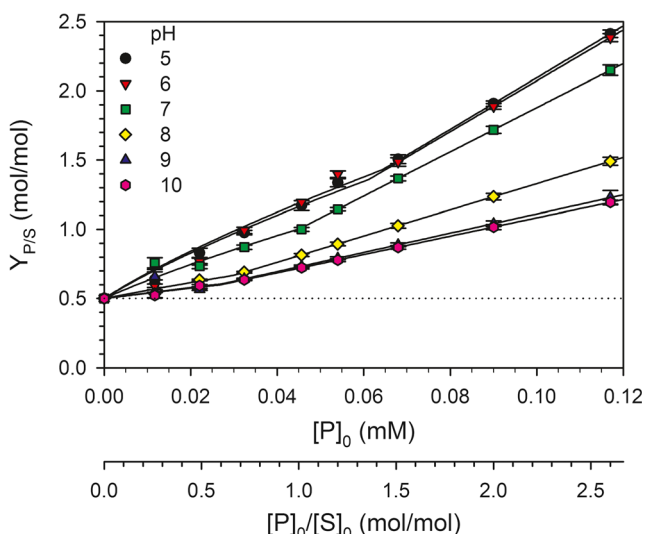


**Fig. 4** Observable stoichiometric coefficient for the HRP-mediated decolourization reaction of OII ( $Y_{P/S}$ ) as a function of the initial hydrogen peroxide concentration ( $[P]_0$ ) corresponding to the different tested pH. In all cases,  $[S]_0 = 0.045$  mM. Bars represent the standard deviation. Lines represent the results of Eqs. (23), (25) and (29) using the coefficients depicted in Table 1. Dotted line indicates the  $Y_{P/S}$  value according to the Dunford mechanism

there was a noticeable effect of the initial hydrogen peroxide concentration on  $Y_{P/S}$ ; within this range of pH,  $Y_{P/S}$  values increased from 0.5 to about 2.4 mol/mol. Thus,  $Y_{P/S}$  values obtained at pHs higher than 8 indicate that the consumption of  $P$  during the decolourization reaction was mainly to oxidize the reducing substrate. Several authors reported a ratio  $Y_{P/S}$  close to 1 mol/mol for the removal of phenol by HRP (Buchanan and Nicell 1997, 1999; Wu et al. 1999; Buchanan and Han 2000). Besides, Chahbane et al. (2007) report  $Y_{P/S}$  values ranging from 1 to 2 mol/mol.

**Effect of the initial hydrogen peroxide and OII concentrations on the initial specific decolourization rate ( $q_0$ ) at different pH**

In addition to stoichiometric issues (“Stoichiometry of the HRP mediated decolourization reaction of OII by hydrogen peroxide ( $Y_{P/S}$ )” section), kinetic features of the HRP-mediated decolourization of OII by hydrogen peroxide is crucial for designing purposes. This section deals

with the effect of the initial concentrations of OII ( $[S]_0$ ), hydrogen peroxide ( $[P]_0$ ) and pH on the initial specific decolourization rate ( $q_0$ ).

Figure 5 shows the effect of initial hydrogen peroxide and dye concentrations on the initial specific decolourization rate ( $q_0$ ) of OII solutions at different pHs. As a general rule, a noticeable increase of  $q_0$  was observed for pH values higher than 7. Additionally, for a given pH,  $q_0$  increased as a function of  $[S]_0$  within the tested range of dye concentrations. Also, there was a noticeable inhibitory effect of high concentrations of hydrogen peroxide on  $q_0$ . Several authors (Gómez et al. 2008; Dunford 2010) associate this inhibitory effect with the formation of an inactive enzyme-peroxide complex at high hydrogen peroxide concentrations. Figure 5 also shows that for a given pH and initial dye concentration, the higher  $q_0$  values were obtained when  $[P]_0$  was around 0.05 mM. In Fig. 6, these observed maximum  $q_0$  values ( $q_{0max}$ ) were plotted as a function of pH, showing that, regardless of  $[S]_0$ , pH had a strong effect on  $q_{0max}$ . As a general rule, a 30-fold increase on the initial specific activity of the HRP was observed when pH increased from 5 to 10. Results shown in Fig. 6 are quite similar to those reported by Chahbane et al. (2007) for the decolourization rate of OII by hydrogen peroxide catalyzed by several biomimetic models of peroxidases. Those authors found a strong increase in the decolourization rate when pH values increased from 5 to 9, with the maximum decolourization rate at pH being between 9 and 10. Considering that  $pK_a$  of OII ( $S$ ) and hydrogen peroxide ( $P$ ) are 11.4 and 11.7, respectively (Oakes and Gratton, 1998), within the tested pH range (5 to 10), both substrates of the HRP were present mainly as their respective non-dissociated species. For this reason, the observed dependence of  $q_{0max}$  as a function of pH was attributed to the presence of, at least, two enzymatic species with a relative distribution that depends on pH, in accordance with the proposed model.

From Eq. (10), the reducing substrate consumption rate ( $V_S$ ) and the decolourization rate ( $V_D$ ) are related as follows (see Supplementary Material, item 4)

$$V_D = (1-r_f)\varepsilon_S V_S \tag{30}$$

Besides, according to Eq. (10) the initial reducing substrate (e.g. OII in this work) consumption rate ( $V_{S0}$ ) is a function of pH and of the initial concentrations of  $S$ ,  $P$  and  $E_T$ :

$$V_{S0} = 2 \left( k_c + k_{ch} \frac{K_{Sh}K_{Ph}}{K_S K_P} \frac{H}{K_a} \right) E_T \frac{K_S K_P [S]_0 [P]_0}{\left( 1 + \frac{H}{K_a} \right) + \left( K_P + K_{Ph} \frac{H}{K_a} \right) [P]_0 + \left( K_P K_I + K_{Ih} K_{Ph} \frac{H}{K_a} \right) [P]_0^2 + \left( K_S K_P + K_{Sh} K_{Ph} \frac{H}{K_a} \right) [S]_0 [P]_0} \tag{31}$$

Combining Eqs. (30) and (31), the initial specific decolourization rate ( $q_0$ , a.u. min<sup>-1</sup> L<sup>-1</sup> mgE<sup>-1</sup>) is

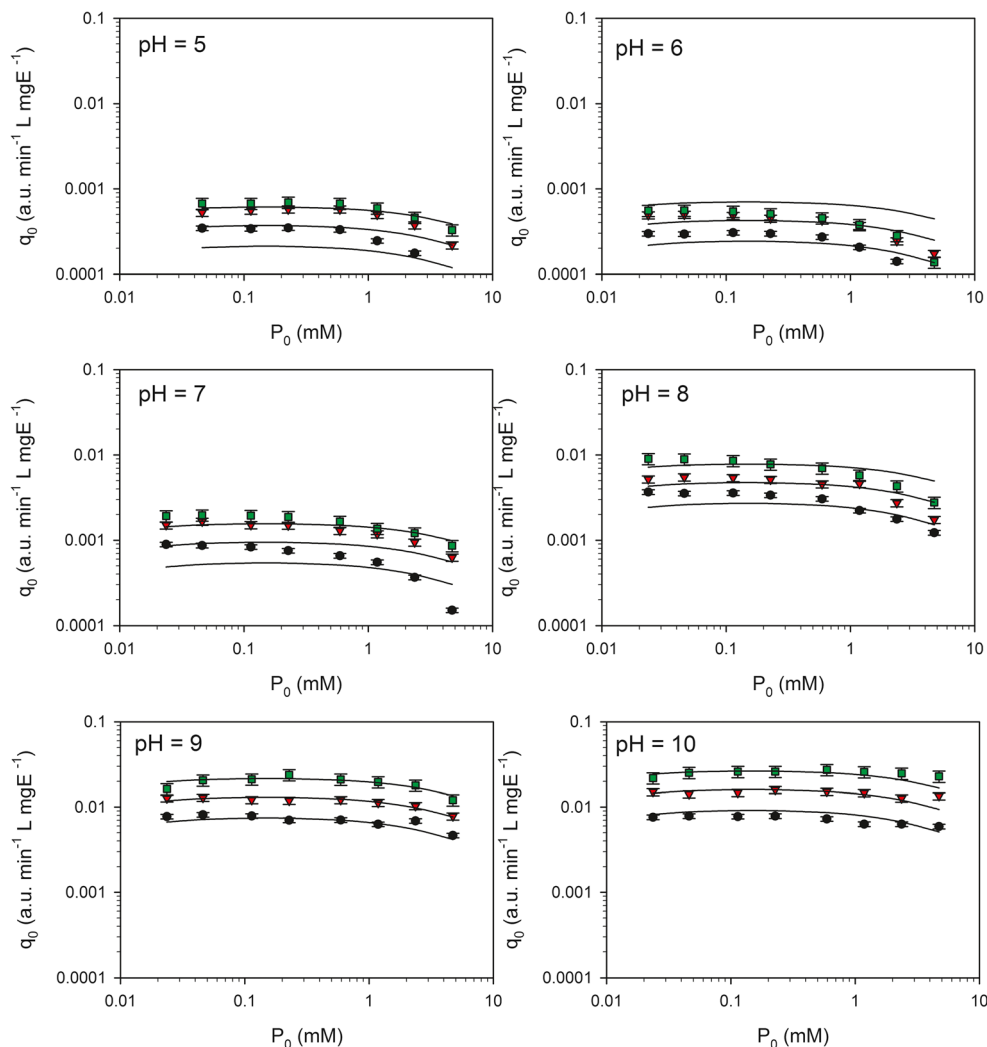
$$q_0 = 2(1-r_f)\varepsilon_S \left( k_c + k_{ch} \frac{K_{Sh}K_{Ph}H}{K_SK_PK_a} \right) \frac{K_SK_P[S]_0[P]_0}{\left( 1 + \frac{H}{K_a} \right) + \left( K_P + K_{Ph} \frac{H}{K_a} \right) [P]_0 + \left( K_PK_I + K_{Ih}K_{Ph} \frac{H}{K_a} \right) [P]_0^2 + \left( K_SK_P + K_{Sh}K_{Ph} \frac{H}{K_a} \right) [S]_0[P]_0} \tag{32}$$

where  $r_f$  is a function of pH (Eq. (20)).

Three different fitting procedures of Eq. (32) to the experimental data were performed. During all fitting procedures,  $r_f$  values were calculated using Eq. (20) along with coefficients shown in Table 1. In the first case (case 1), the whole Eq. (32) was fitted to the experimental  $q_0$  values obtained at different initial concentrations of S (0.02–0.09 mM), P (0.02–4.7 mM) and pH (5–10). Although a quite satisfactory fit of Eq. (31) to the experimental data was obtained, the coefficient of

variation corresponding to  $K_{Ph}$  was 166% (Table 2), suggesting an overparameterization of this equation. For this reason, in case 2, it was assumed that  $K_{Ph} = K_P$ . This approximation did not produce an increase in the root mean square error (RMSE) with respect to case 1, confirming the overparameterization of Eq. (32) to represent the experimental data within the tested conditions. Moreover, in case 2, several fitted coefficients had a lower coefficient of variation with respect to case 1 (Table 2). In an attempt to further simplify Eq. (32), in case

**Fig. 5** Effect of initial hydrogen peroxide ( $P_0$ ) and dye ( $S_0$ ) concentrations on the initial specific decolourization rate ( $q_0$ ) of OII solutions at different pH values.  $[S]_0$  values were 0.023 mM (black circles), 0.045 mM (red triangles) and 0.090 mM (green squares). Bars represent the standard deviation. Lines represent the proposed model (Eq. 32, case 2) using the coefficients shown in Tables 1 and 2



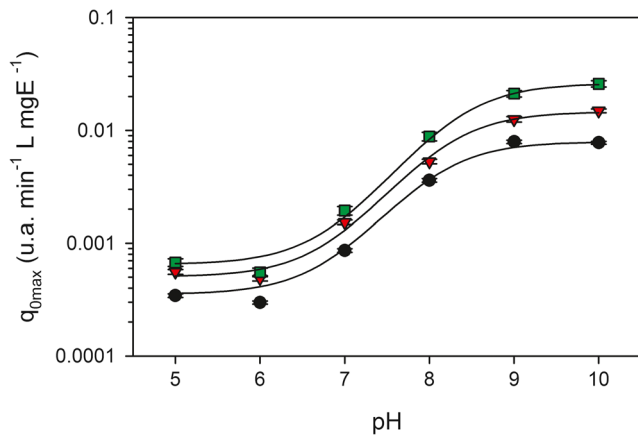


**Fig. 6** Effect of pH on the observed maximum initial specific decolourization rate ( $q_{0max}$ ) of OII solutions at different pH values.  $[S]_0$ : 0.023 mM (black circles), 0.045 mM (red triangles) and 0.090 mM (green squares). Bars represent the standard deviation. Lines represent the proposed model (Eq. 32, case 2) assuming  $[P]_0 = 0.05$  mM along with the coefficients shown in Tables 1 and 2

3 it was assumed that  $K_{Ph} = K_P$  and  $K_{Sh} = K_S$ . Although fitted as a function of experimental  $q_0$  values for all cases were quite similar (Supplementary Material, Figs. S2 to S5), RMSE corresponding to case 3 increased by about 20% with respect to case 2 (Table 2). Besides, while 76% of the calculated  $q_0$  using cases 1 and 2 had a relative error lower than 20%, this value was 67% for case 3 (Fig. SD6).

**Reuse of the enzyme and validation of the proposed model**

Figures 5 and 6 show that case 2 of the proposed model adequately represents the initial specific decolourization rate ( $q_0$ ) for all the tested conditions. However, it must be noted that in those experiments a single use of the enzyme was performed. Taking into account that HRP is a relatively expensive enzyme, it would be desirable to reuse it as much as possible. To asses the possibility of reusing the HRP, repeated additions

**Table 2** Fitting results of Eq. (32) to the data depicted in Fig. 5. In all cases,  $\epsilon_S = 19.5$  a.u.  $cm^{-1} mM^{-1}$ ,  $H = 10^{-pH}$  and  $r_f$  were obtained from Eq. (20) using the coefficients shown in Table 1

Case	Coefficient	Value	Std. error	CV (%)	RMSE	$r^2$			
(1) Full equation	$k_c$ (mmol P $mgE^{-1} min^{-1}$ ) <sup>a</sup>	$3.3 \times 10^{-3}$	$0.4 \times 10^{-3}$	12.1	$3.50 \times 10^{-4}$	0.992			
	$K_S$ ( $mM^{-1}$ )	3.2	0.5	15.6					
	$K_P$ ( $mM^{-1}$ )	308	100	32.5					
	$K_I$ ( $mM^{-1}$ )	0.05	0.01	20.0					
	$pK_a$	8.0	0.7	11.4					
	$k_{ch}$ (mmol P $mgE^{-1} min^{-1}$ ) <sup>a</sup>	$2.6 \times 10^{-5}$	$0.3 \times 10^{-5}$	11.5					
	$K_{Sh}$ ( $mM^{-1}$ )	32	9	28.1					
	$K_{Ph}$ ( $mM^{-1}$ )	267	400	150					
	$K_{Ih}$ ( $mM^{-1}$ )	1.8	0.4	22.2					
	(2) $K_{Ph} = K_P$	$k_c$ (mmol P $mgE^{-1} min^{-1}$ ) <sup>a</sup>	$3.3 \times 10^{-3}$	$0.4 \times 10^{-3}$			12.1	$3.50 \times 10^{-4}$	0.992
		$K_S$ ( $mM^{-1}$ )	3.2	0.5			15.6		
$K_P$ ( $mM^{-1}$ )		304	90	29.3					
$K_I$ ( $mM^{-1}$ )		0.05	0.01	20.5					
$pK_a$		7.89	0.07	0.9					
$k_{ch}$ (mmol P $mgE^{-1} min^{-1}$ ) <sup>a</sup>		$2.7 \times 10^{-5}$	$0.3 \times 10^{-5}$	11.1					
$K_{Sh}$ ( $mM^{-1}$ )		32	7	21.9					
$K_{Ph}$ ( $mM^{-1}$ )		304	–	–					
$K_{Ih}$ ( $mM^{-1}$ )		1.8	0.3	16.7					
(3) $K_{Ph} = K_P$ $K_{Sh} = K_S$		$k_c$ (mmol P $mgE^{-1} min^{-1}$ ) <sup>a</sup>	$2.1 \times 10^{-3}$	$0.2 \times 10^{-3}$	9.5	$4.21 \times 10^{-4}$	0.988		
		$K_S$ ( $mM^{-1}$ )	5.6	0.6	10.7				
	$K_P$ ( $mM^{-1}$ )	345	100	29.0					
	$K_I$ ( $mM^{-1}$ )	0.06	0.01	16.7					
	$pK_a$	8.27	0.02	0.2					
	$k_{ch}$ (mmol P $mgE^{-1} min^{-1}$ ) <sup>a</sup>	$6.9 \times 10^{-5}$	$0.7 \times 10^{-5}$	10.1					
	$K_{Sh}$ ( $mM^{-1}$ )	5.6	–	–					
	$K_{Ph}$ ( $mM^{-1}$ )	345	–	–					
	$K_{Ih}$ ( $mM^{-1}$ )	0.9	0.1	11.1					

RMSE root mean square error

<sup>a</sup> The units corresponding to  $k_c$  and  $k_{ch}$  are millimoles of P  $mgE^{-1} min^{-1}$  because the number “2” in Eq. (32) indicates that 2 mol of S is oxidized per mol of P consumed during the decolourization reactions. For this reason, this number is not a dimensionless one but has the following units: mol S/mol P. Besides, note that these units are also in accordance with Eq. (22)

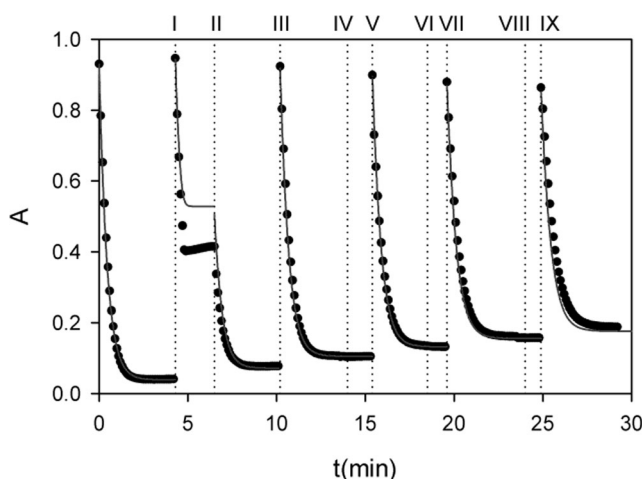


**Fig. 7** Absorbance at 485 nm (black symbols) as a function of time during repeated additions of 0.05 mL of Orange II (2 mM) (runs I, III, V, VII, X) and 0.1 mL of hydrogen peroxide (2 mM) (runs II, IV, VI, VIII). Initial conditions:  $[E_T]_0 = 143$  mgE/L,  $[S]_0 = [P]_0 = 0.048$  mM, pH = 9, volume of mixture reaction = 2.1 mL. Dotted lines indicate each run. Continuous line represents the proposed model (Eqs. 10 to 13, 20, 23) along with the coefficients shown in Tables 1 and 2 (case 2). For more details see Supplementary Material, item 5

of OII and hydrogen peroxide were performed to the same reaction mixture (Fig. 7).

The experiment started as a typical batch assay with the following initial conditions:  $[E_T]_0 = 143$  mgE/L,  $[S]_0 = [P]_0 = 0.048$  mM, pH = 9, volume of mixture reaction = 2.1 mL. Figure 7 shows that under these conditions a fast decolourization occurred. At 4.3 min, a new pulse of 0.05 mL of OII (2 mM) was added to the reaction mixture (Fig. 7, run I). The absorbance decreased from 0.95 to 0.41 in about 1 min and then remained constant, suggesting the absence of hydrogen peroxide. For this reason, at 6.5 min 0.10 mL of P (2 mM) was added (Fig. 7, run II) and the absorbance decreased to 0.08 in a minute, confirming that the decolourization in run I stopped due to the complete consumption of P. Then, in runs III to IX, consecutive additions of 0.05 mL of OII (2 mM) and 0.10 mL of P (2 mM) were performed. According to Fig. 7, the enzyme remained active after six reuse cycles, demonstrating that under the tested conditions the deactivation of the enzyme was negligible, as it was assumed to develop the model proposed in the present work (“Modified Dunford mechanism” section 1.2). Moreover, Fig. 7 shows a slow increase of the final absorbance at the end of each run due to the accumulation of OP refractory to decolourization. It must be noted that the above mentioned operation mode (e.g. the repeated additions of OII and P to a similar reaction mixture) is similar to the operation of a fed batch. Thus, Fig. 7 demonstrates that a fed batch could be effective in the decolourization of wastewater containing azo-dyes.

Finally, the model developed in the present work along with the coefficients shown in Tables 1 and 2 was used to

represent the change of the absorbance during the fed batch-type experiment (for details, see Supplementary Material, item 5). Figure 7 shows that the developed model represented quite well the change of the absorbance during these experiments. Considering that this set of data was not used during the fitting procedure of the model, the agreement between predicted and experimental data provides a powerful validation of the model developed in the present work. Moreover, because hydrogen peroxide and the enzyme are directly related with the operational cost, the model developed in the present work can help designers in reducing such costs.

## Conclusions

In this work, a modified version of the classic Dunford mechanism of peroxidases was developed. The proposed model adequately represents the inhibition of the enzymatic activity by high concentrations of hydrogen peroxide (P), the substrate-dependant catalytic activity of peroxidases (e.g. the decomposition of P to water and oxygen) and the effect of pH on the generation of oxidation products (OP) and on the decolourisation kinetics of the azo-dye Orange II (OII) by a horseradish peroxidase (HRP). Obtained results demonstrate that at pH 9–10 and low initial P concentration, the consumption of P was mainly to oxidize OII. Conversely, the catalytic activity prevails at lower pH values and higher P concentrations. Moreover, under acidic conditions, a strong inhibition of the initial specific decolourisation rate ( $q_0$ ) was observed.

Repeated additions of OII and P performed to the same reaction mixture showed that the tested enzyme remained active after six reuse cycles, indicating that under the studied conditions its deactivation was negligible. A satisfactory accordance between the change of the absorbance during these experiments and the absorbances calculated using the fitted model was obtained. Taking into account that hydrogen peroxide and enzyme are directly related with the operational costs, the model developed in the present work can help designers in reducing such costs.

**Acknowledgements** The authors gratefully acknowledge the financial support from Consejo Nacional de Investigaciones Científicas y Técnicas (CONICET), by Universidad Nacional de la Plata (UNLP) and by Agencia Nacional de Promoción Científica y Tecnológica (ANPCyT), Argentina.

**Nomenclature** A, absorbance;  $A_f$ , absorbance at the end of the a decolourization experiment;  $A_{\min}$ , minimum absorbance obtained under the excess of hydrogen peroxide; E, dissociated form of the enzyme;  $E_0$ , resting state of the enzyme;  $E_1$ , compound I of the enzyme;  $E_2$ , compound II of the enzyme; HE, non-dissociated form of the enzyme; HRP, horseradish peroxidase; OII, Orange II; OP, oxidation products of Orange II; P, hydrogen peroxide;  $P_C$ , critical hydrogen peroxide concentration;  $q_0$ , initial specific decolourization rate; S, reducing substrate;  $V_{S0}$ , initial

reducing substrate consumption rate;  $V_{DO}$ , initial decolourization rate;  $V_S$ , reducing substrate consumption rate;  $V_D$ , decolourization rate;  $X$ , oxidation products obtained at basic conditions;  $Y$ , oxidation products obtained at acid conditions;  $Y_{P/S}$ , observable stoichiometric coefficient of decolourization

## References

- Ali L, Algaithi R, Habib HM, Souka U, Rauf MA, Ashraf SS (2013) Soybean peroxidase-mediated degradation of an azo dye- a detailed mechanistic study. *BMC Biochem* 14:35–41
- Buchanan ID, Han YS (2000) Assessment of the potential of *Arthromyces ramosus* peroxidase to remove phenol from industrial wastewaters. *Environ Technol* 21:545–552
- Buchanan ID, Nicell JA (1997) Model development for horseradish peroxidase catalyzed removal of aqueous phenol. *Biotechnol Bioeng* 54:251–261
- Buchanan ID, Nicell JA (1999) A simplified model of peroxidase-catalyzed phenol removal from aqueous solution. *J Chem Technol Biotechnol* 74:669–674
- Cabrera C, Cornaglia A, Córdoba A, Magario I, Ferreira ML (2017) Kinetic modelling of the hematin catalysed decolourization of Orange II solutions. *Chem Eng Sci* 161:127–137
- Chahbane N, Popescu DL, Mitchell DA, Chanda A, Lenoir D, Ryabov AD, Schramma KW, Collins TJ (2007) FeIII-TAML-catalyzed green oxidative degradation of the azo dye Orange II by H<sub>2</sub>O<sub>2</sub> and organic peroxides: products, toxicity, kinetics, and mechanisms. *Green Chem* 9:49–57
- Cheng XB, Jia R, Li PS, Tu SQ, Zhu Q, Tang WZ, Li XD (2007) Studies on the properties and co-immobilization of manganese peroxidase. *Enzym Microb Technol* 41:258–264
- Chiong T, Lau S, Lek ZH, Koh BY, Danquah MK (2016) Enzymatic treatment of methyl orange dye in synthetic wastewater by plant-based peroxidase enzymes. *J Environ Chem Eng* 4:2500–2509
- Darwesh OM, Matter IA, Eida MF (2016) Application of nanotechnology to stabilize peroxidase enzyme and improve it in textile dyes removal from wastewater. Conference proceedings of the 7<sup>th</sup> International Conference on Water Resources and Arid Environments (ICWRAE 7), pp 465–473
- Doumic LI, Haure PA, Cassanello MC, Ayude MA (2013) Mineralization and efficiency in the homogeneous Fenton Orange G oxidation. *Appl Catal B Environ* 142–143:214–221
- Doumic LI, Salierno G, Cassanello MC, Haure PA, Ayude MA (2015) Efficient removal of Orange G using Prussian Blue nanoparticles supported over alumina. *Catal Today* 240:67–72
- Dükkancı M, Vinatoru M, Mason TJ (2014) The sonochemical decolourization of textile azo dye Orange II: effects of Fenton type reagents and UV light. *Ultrason Sonochem* 21:846–853
- Dunford HB (2010) Horseradish peroxidase. II. Two-electron reactions, ferrous peroxidase, compound III, the five oxidation states, oxygen evolution and inactivation. In: Dunford HB (ed) *Peroxidases and catalases: Biochemistry, biophysics, biotechnology, and physiology*, 2nd edn. Wiley, New Jersey, pp 41–57
- Dunford HB, Stillman JS (1976) On the function and mechanism of action of peroxidases. *Coord Chem Rev* 19:187–251
- Forgacs E, Cserhatia T, Oros G (2004) Removal of synthetic dyes from wastewaters: a review. *Environ Int* 30:953–971
- Franciscon E, Piubeli F, Garboggini FF, De Menezes CR, Silva IS, Paulo AC, Grossman MJ, Durrant LR (2010) Polymerization study of the aromatic amines generated by the biodegradation of azo dyes using the laccase enzyme. *Enzym Microb Technol* 46:360–365
- Frey PA, Hegeman AD (2007) *Enzymatic reaction mechanisms*. Oxford University Press, Inc, Oxford
- Gómez JL, Bódalo A, Gómez E, Bastida J, Hidalgo AM, Gómez M (2008) A covered particle deactivation model and an expanded Dunford mechanism for the kinetic analysis of the immobilized SBP/phenol/hydrogen peroxide system. *Chem Eng J* 138:460–473
- Inchaurrondo N, Font J, Ramos CP, Haure P (2016) Natural diatomites: efficient green catalyst for Fenton-like oxidation of Orange II. *Appl Catal B Environ* 181:481–494
- Jakopitsch C, Wanasinghe A, Jantschko W, Furtmuller PG, Obinger C (2005) Kinetics of interconversion of ferrous enzymes, compound II and compound III, of wild-type *Synechocystis* catalase-peroxidase and Y249F. Proposal for the catalytic mechanism. *J Biol Chem* 280(10):9037–9042
- Kalsoom U, Ashraf SS, Meetani MA, Rauf MA, Bhatti HN (2013) Mechanistic study of a diazo dye degradation by soybean peroxidase. *Chem Cent J* 7:1–10
- Lau Y-Y, Wong Y-S, Teng T-T, Morad N, Rafatullah M, Ong S-A (2014) Coagulation-flocculation of azo dye Acid Orange 7 with green refined laterite soil. *Chem Eng J* 246:383–390
- Li F, Li G, Zhang X (2014) Mechanism of enhanced removal of quinonic intermediates during electrochemical oxidation of Orange II under ultraviolet irradiation. *J Environ Sci* 26:708–715
- Lin H, Zhang H, Wang X, Wang L, Wu J (2014) Electro-Fenton removal of Orange II in a divided cell: reaction mechanism, degradation pathway and toxicity evolution. *Sep Purif Technol* 122:533–540
- Lopez C (2005) Oxidación del tinte azo Orange II mediante MnP en reactores enzimáticos operados en continuo. Ph.D. Thesis. Universidade de Santiago de Compostela. Santiago de Compostela
- Lopez C, Valade AG, Combourieu B, Mielgo I, Bouchon B, Lema JM (2004) Mechanism of enzymatic degradation of the azo dye Orange II determined by ex situ <sup>1</sup>H nuclear magnetic resonance and electrospray ionization-ion trap mass spectrometry. *Anal Biochem* 335:135–149
- Mo JH, Lee YH, Kim J, Jeong JY, Jegal J (2008) Treatment of dye aqueous solutions using nanofiltration polyamide composite membranes for the dye wastewater reuse. *Dyes Pigments* 76: 429–434
- Nicell JA, Wright H (1997) A model of peroxidase activity with inhibition by hydrogen peroxide. *Enzym Microb Technol* 21:302–310
- Oakes J, Gratton P (1998) Kinetic investigations of azo dye oxidation in aqueous media. *J Chem Soc Perkin Trans 2*:1857–1864
- Olsen LF, Hauser MJB, Kummer U (2003) Mechanism of protection of peroxidase activity by oscillatory dynamics. *Eur J Biochem* 270: 2796–2804
- Rache ML, García AR, Zea HR, Silva AMT, Madeira LM, Ramirez JH (2014) Azo-dye orange II degradation by the heterogeneous Fenton-like process using a zeolite Y-Fe catalyst—kinetics with a model based on the Fermi's equation. *Appl Catal B Environ* 146:192–200
- Rauf MA, Ashraf SS (2012) Survey of recent trends in biochemically assisted degradation of dyes. *Chem Eng J* 209:520–530
- Sahare P, Ayala M, Vazquez-Duhalt R, Pal U, Loni A, Canham LT, Osorio I, Agarwal V (2016) Enhancement of peroxidase stability against oxidative self-inactivation by co-immobilization with a redox-active protein in mesoporous silicon and silica microparticles. *Nanoscale Res Lett* 11:417–427
- Saratale RG, Saratale GD, Chang JS, Govindwar SP (2011) Bacterial decolorization and degradation of azo dyes: a review. *J Taiwan Inst Chem Eng* 42:138–157
- Satar R, Husain Q (2009) Applications of Celite-adsorbed white radish (*Raphanus sativus*) peroxidase in batch process and continuous reactor for the degradation of reactive dyes. *Biochem Eng J* 46:96–104
- Sudha M, Saranya A, Selvakumar G, Sivakumar N (2014) Microbial degradation of azo dyes: a review. *Int J Curr Microbiol App Sci* 3(2):670–690

- Tijsskens LMM, Greiner R, Biekman ESA, Konietzny U (2001) Modeling the effect of temperature and pH on activity of enzymes: the case of phytases. *Biotechnol Bioeng* 72(3):323–330
- Tizaouiia C, Grima N (2011) Kinetics of the ozone oxidation of reactive Orange 16 azo-dye in aqueous solution. *Chem Eng J* 173:463–473
- Wu J, Taylor KE, Biswas N, Bewtra JK (1999) Kinetic model for removal of phenol by horseradish peroxidase with PEG. *J Environ Eng* 125: 451–458
- Zhang L, Chen L, Liu X, Zhang W (2015) Effective removal of azo-dye orange II from aqueous solution by zirconium-based chitosan microcomposite adsorbent. *RSC Adv* 5:93840–93849
- Zhou G, Guo J, Zhou G, Wan X, Shi H (2016) Photodegradation of Orange II using waste paper sludge-derived heterogeneous catalyst in the presence of oxalate under ultraviolet light emitting diode irradiation. *J Environ Sci* 47:63–70